

Magnetic Properties of the Thin Films of Prussian Blue Analogues Obtained by Ion-Exchange Synthesis

W. SAS^{a,b}, A. PACANOWSKA^a AND M. FITTA^{a,*}

^a*Institute of Nuclear Physics Polish Academy of Sciences, Radzikowskiego 152, 31-342 Kraków, Poland*

^b*Institute of Physics, Bijenička 46, 10000 Zagreb, Croatia*

Doi: [10.12693/APhysPolA.145.109](https://doi.org/10.12693/APhysPolA.145.109)

*e-mail: magdalena.fitta@ifj.edu.pl

The Prussian blue analogues attract great attention due to their interesting properties and tunability. The cyanido bridging ligands allow for effective magnetic coupling. Due to the highly symmetrical structure of the Prussian blue analogue, its properties can be tuned by changing the metal centres involved in the cyano-bridging. Herein, a study of a new dimensionally-reduced system based on nickel hexacyanoferrate/chromate is presented. Thin films were obtained by ion-exchange synthesis. The primary aim of this work was to tune the physical properties of Prussian blue analogues by adapting the strategy of incorporating the three types of metal ions. A comprehensive analysis of the magnetic properties of the resulting compound and a detailed investigation of the evolution of the material's microstructure induced by the change in its chemical composition is presented.

topics: molecular magnetism, thin films, Prussian blue analogues

1. Introduction

The Prussian blue analogues (PBAs) $A_jM'_k[M(CN)_6]_l \cdot nH_2O$, where M' and M are 3d transition metal ions and A is an interstitial cation, attract great attention due to their rich palette of properties such as room-temperature ferromagnetism [1, 2], photomagnetism [3, 4], magnetic sensitivity to external pressure [5, 6], and the negative thermal expansion [7]. Thin films of PBAs are therefore considered as interesting materials for power supply and storage [8–11], ion-sieving membranes [12], or future molecule-based spintronic devices [13, 14]. One of the most important advantages of PBAs is their highly symmetrical structure. Depending on the stoichiometry and the charge of the cation, these systems reveal different structural motifs based on the highly symmetric, regular, and three-dimensional coordination network. Due to the cubic structure, the properties of PBAs can be tuned by changing the metal centres involved in the cyano-bridging.

One of the first examples of Prussian blue analogues composed of three types of metal ions was the mixed ferromagnet–ferrimagnet $(Ni^II_xMn^II_{1-x})_{1.5}[Cr^III(CN)_6] \cdot 7.5H_2O$, which accommodated both ferromagnetic ($J > 0$) and antiferromagnetic ($J < 0$) exchange interactions [15]. For that series of compounds, obtained as a microcrystalline powder, a monotonous increase

in Weiss temperature with the increase in nickel content was observed. Variation in structural and magnetic properties with composition was also reported for the $(Co_xNi_{1-x})_{1.5}[Fe(CN)_6] \cdot zH_2O$ series [16]. Next, the tunability of physical properties by controlling the compositional factor x was also achieved for thin films of $(Fe^II_xCr^II_{1-x})_{1.5}[Cr^III(CN)_6] \cdot zH_2O$ [17] and $(V^{II/III}_xCr^II_{1-x})_{1.5}[Cr^III(CN)_6]_y$ [18] synthesized by electrochemical deposition. Depending on the x value, the change in colour, critical temperature, and coercive field of the films were noted. The influence of metal components on the spectroscopic and magnetic properties was also demonstrated for cobalt hexacyanoferrate/chromate metal coordination nanopolymers [19].

The objective of the present work was to design and optimize a feasible and reproducible process for the synthesis of thin films from the PBAs family with tuned magnetic properties. The stoichiometry of the systems studied changes from $Ni_3[Cr(CN)_6]_2$ to $Ni_3[Fe(CN)_6]_2$ depending on the $[Cr(CN)_6]^{3-}:[Fe(CN)_6]^{3-}$ ratio, but the $Ni_3[M(CN)_6]_2$ core is maintained. The structure of the system reveals the face-center-cubic packing, thus allowing the formation of cyano linkages between Ni^{2+} cations and hexacyanometallate. In our previous paper [20], we have already reported on the synthesis and magneto-optical properties of $Ni_{1.5}[Fe(CN)_6]_x[Cr(CN)_6]_{1-x} \cdot nH_2O$ ($x=0, 0.55,$

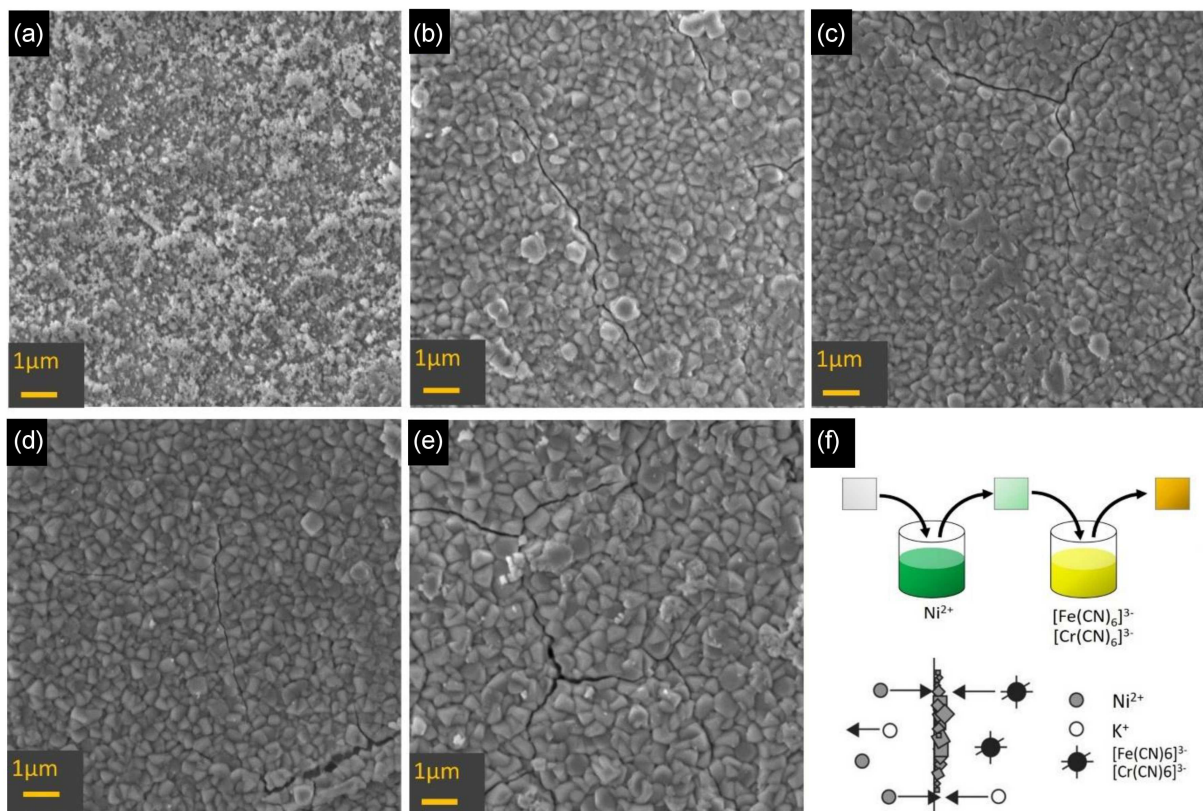


Fig. 1. SEM images of the films with various values of the compositional x factor (a) $x = 0$, (b) $x = 0.31$, (c) $x = 0.57$, (d) $x = 81$, and (e) $x = 1$. (f) The scheme of ion exchange deposition of PBA thin film.

and 1) thin films grown on silicon (100) and mica substrates. Now, we present thin film samples of the same family with the assumed x values as $x_{ass} = 0, 0.25, 0.5, 0.75$, and 1, deposited onto the Nafion®117 membrane. The effectiveness and composition accuracy of the film preparation technique were checked by scanning electron microscope (SEM), energy-dispersive X-ray spectroscopy (EDS), and magnetic measurements.

2. Materials and methods

2.1. Sample preparation

All reagents used in this study were purchased from commercial sources (Sigma-Aldrich) and used without further purification. In the first step of the film preparation by ion-exchange synthesis, a Nafion®117 membrane ($1 \times 2 \text{ cm}^2$) was immersed in an aqueous solution of NiCl_2 (200 mM) for 24 h. Then, it was rinsed with deionized (DI) water and placed in an aqueous solution of $\text{K}_3[\text{Fe}(\text{CN})_6]$ and/or $\text{K}_3[\text{Cr}(\text{CN})_6]$. The compositional factor x , $x = n_{\text{Cr}}/(n_{\text{Cr}} + n_{\text{Fe}})$, was varied from 0 to 1, keeping the total potassium hexacyanometalate concentration of 20 mmol. After completion of the synthesis, all membranes were washed again with deionized water and allowed to dry in ambient air.

2.2. Characterization methods

Microstructure and composition analysis of films was performed using a TESCAN VEGA3 scanning electron microscope equipped with an X-ray energy dispersive spectrometer EDAX Bruker.

Magnetic properties were measured using a Quantum Design MPMS-XL magnetometer. For magnetic measurements, the samples deposited on Nafion®117 were cut into pieces ca. $3 \times 4 \text{ mm}^2$ in size, and subsequently, they were introduced into the sample holder oriented parallel to the applied magnetic field. For reference, the magnetic properties of the Nafion®117 substrate were measured independently under the same conditions and then subtracted from the raw data.

3. Results and discussion

3.1. SEM

The chemical composition of the thin films was determined by means of SEM and EDS. No fewer than three scans were recorded on different parts of each film and then averaged to give relative atomic percentages for the metallic elements. The calculated transition metal ratios are presented in Table I. Results of the elemental analysis showed

TABLE I
The chemical composition of $\text{Ni}_{1.5}[\text{Fe}(\text{CN})_6]_x[\text{Cr}(\text{CN})_6]_{1-x} \cdot n\text{H}_2\text{O}$ films deposited on Nafion®117.

x_{ass}	x	Ni [%]	Fe [%]	Cr [%]
0	0	33.5 ± 1.1	–	60.19 ± 0.88
0.25	0.31	30.7 ± 2.0	21.5 ± 1.0	47.8 ± 1.2
0.5	0.57	30.78 ± 0.74	39.32 ± 0.30	29.90 ± 0.80
0.75	0.81	31.3 ± 1.2	55.48 ± 0.88	13.27 ± 0.44
1	1	24.9 ± 2.8	75.1 ± 2.8	–

that the experimentally obtained x values are close to the x_{ass} assumed in the synthesis protocol, e.g., $x = 0.31$ ($x_{ass} = 0.25$), $x = 0.57$ ($x_{ass} = 0.50$), and 0.81 ($x_{ass} = 0.75$).

The surface morphology was examined by SEM. Figure 1 shows the microphotographs obtained for exemplary films. The morphology of the films consists of a collection of crystallites formed on the surface. The smallest crystallites were obtained for the NiCr sample, and their sizes do not exceed 100 nm. The grains are much larger (with diameters in the range of 600 to 800 nm) for samples with the highest Fe content. A reverse relationship has already been observed for PBA films obtained by “layer by layer” deposition, where films based on nickel hexacyanoferrate contain slightly smaller granules than hexacyanochromate films [21]. Another characteristic feature of PBA films observed in the SEM images are cracks seen on the surface.

3.2. Magnetic properties

It has also been demonstrated that the magnetic properties of the thin films depend on the metal elemental composition. Figure 2a shows the temperature dependence of the real component of the AC susceptibility measured for the films oriented parallel to the direction of an external magnetic field. For all compounds, sharp peaks are observed, revealing the presence of a long-range magnetic ordering below the respective critical temperatures. The critical temperatures T_c , determined as a minimum of χ' derivative, are equal to 26.6 K, 30.8 K, 40.4 K, 52.7 K, and 64 K for $x = 1, 0.81, 0.57, 0.31,$ and 0 , respectively. This means that the ordering temperature is shifted to the higher values with the decrease in Fe content in the samples.

Figure 2b shows the results of field-cooled (FC) magnetization measurements recorded for samples with the external magnetic field (100 Oe) applied parallel to the surface of the films. For all compounds, during cooling, the magnetic susceptibility increases slowly, then the signal goes up abruptly when passing the critical temperature, and finally, it saturates at low temperatures.

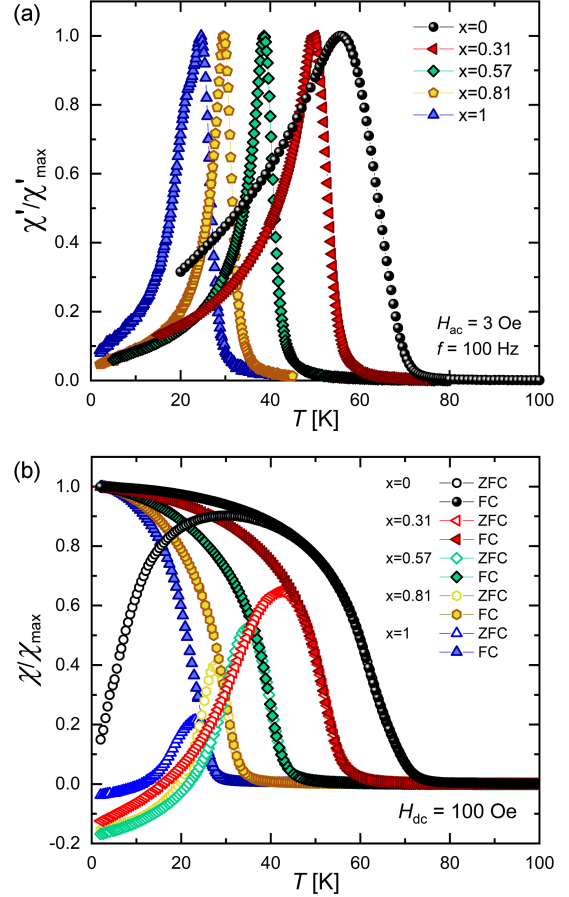


Fig. 2. (a) Temperature dependence of real component of AC susceptibility measured for films obtained with various values of the compositional x factor, oriented parallel to the direction of H_{dc} . (b) ZFC–FC magnetization vs temperature plots measured at an applied field of 100 Oe for films aligned parallel to the external field direction.

For all films with $x > 0$, the negative values of magnetization in the low-temperature range in the zero-field-cooling (ZFC) curve are observed. Typically, the occurrence of a negative magnetization value in $M(T)$ curves is associated with the compensation point, where the algebraic sum of sublattice magnetizations equals zero. The compensation temperature is anticipated to be independent of the external field magnitude. The presence of this compensation temperature has been observed in various PBA samples, both in bulk and thin films. In our case, all analyzed compounds are anticipated to exhibit ferromagnetic behaviour, then the negative magnetization may possibly be related to the presence of some negative remnant field of the superconducting magnet. A similar effect was previously observed for PBA thin films obtained by layer-by-layer deposition. Therefore, these deviations should be treated as measurement artifacts and not as an additional physical effect originating from the samples.

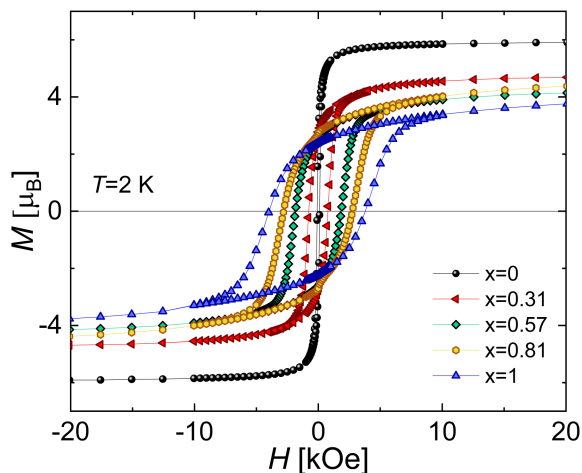


Fig. 3. Magnetization vs field measured at 2 K for $\text{Ni}_{1.5}[\text{Fe}(\text{CN})_6]_x[\text{Cr}(\text{CN})_6]_{1-x} \cdot n\text{H}_2\text{O}$ films.

TABLE II
Magnetic data for the $\text{Ni}_{1.5}[\text{Fe}(\text{CN})_6]_x[\text{Cr}(\text{CN})_6]_{1-x} \cdot n\text{H}_2\text{O}$ thin film samples.

x	T_c [K]	H_c [Oe]	M_s [μ_B]	θ [K]	C [emu K/mol]
0	64	100	5.9	81.56	4.19
0.31	52.7	770	4.78	67.86	3.46
0.57	40.4	1850	4.31	56.69	2.99
0.81	30.8	2780	4.66	46.64	3.03
1	26.6	3890	4.15	23.67	3.16

Additionally, the static magnetic susceptibility was measured for all of the films in the presence of the field of 500 Oe. Fitting the Curie–Weiss law to the experimental data in the form of $1/\chi(T)$ vs T in the temperature range 100–300 K gives the Curie constants and Weiss temperatures listed in Table II. The values of C as well as θ_{CW} increase monotonically with the increase in Cr content. Positive values of Weiss temperature determined for all films confirm the presence of ferromagnetic interaction between metal ions.

Figure 3 presents the dependence of the coercive field and critical temperature on the value of x . It is clearly seen that H_c , as well as T_c , changes monotonically with the change of parameter x . An increase in Fe content leads to an increase in the coercive field, whereas the critical temperature decreases. Taking into account the spin values $s_{\text{Ni}} = 1$, $s_{\text{Fe}} = 1/2$, $s_{\text{Cr}} = 3/2$, and $g = 2$, the theoretical saturation of magnetization of the $\text{Ni}_{1.5}[\text{Fe}(\text{CN})_6]_x[\text{Cr}(\text{CN})_6]_{1-x} \cdot n\text{H}_2\text{O}$ series should change from $6 \mu_B$ ($x = 0$) to $4 \mu_B$ ($x = 1$). The experimentally obtained values of M_s are close to those predicted theoretically. It means that the control of the Fe/Cr ratio allows for tuning the desired magnetic properties of the obtained compounds.

The magnetic properties of deposited films are comparable to their bulk counterparts; in fact, small discrepancies between values of T_c , H_c , and M_s may be related to slightly different sample stoichiometry.

4. Conclusions

The development of modern science and technology requires novel and tunable magnetic materials. In this work, we have succeeded in designing a series of magnetic thin films composed of new types of PBAs incorporating three types of metal ions. The proper film formation and composition have been confirmed with the use of the EDS technique. The physical properties of the obtained films can be controlled by changing the compositional x factor. It has been demonstrated that the coercive field H_c , as well as the critical temperature T_c , changes monotonically with the change of the x parameter. An increase in the Fe content leads to a decrease in the critical temperature, whereas the coercive field increases. Moreover, our results show that the films' magnetic properties are compatible with their bulk counterpart.

References

- [1] S. Ferlay, T. Mallah, R. Ouahčs, P. Veillet, M. Verdaguer, *Nature* **378**, 701 (1995).
- [2] J.M. Manriquez, G.T. Yee, R.S. McLean, A.J. Epstein, J.S. Miller, *Science* **252**, 1415 (1991).
- [3] T. Yamamoto, Y. Umemura, O. Sato, Y. Einaga, *Chem. Lett.* **33**, 500 (2004).
- [4] H. Tokoro, T. Matsuda, T. Nuida, Y. Moritomo, K. Ohoyama, E.D.L. Dangui, K. Boukheddaden, S. Ohkoshi, *Chem. Mater.* **20**, 423 (2008).
- [5] E. Coronado, M.C. Giménez-López, G. Levchenko, F.M. Romero, V. García-Baonza, A. Milner, M. Paz-Pasternak, *J. Am. Chem. Soc.* **127**, 4580 (2005).
- [6] M. Zentková, Z. Arnold, J. Kamarád, V. Kavečanský, M. Lukáčová, S. Matáš, M. Mihalik, Z. Mitróová, A. Zentko, *J. Phys. Condens. Matter* **19**, 266217 (2007).
- [7] K.W. Chapman, P.J. Chupas, C.J. Kepert, *J. Am. Chem. Soc.* **128**, 7009 (2006).
- [8] L. Zhang, T. Meng, B. Mao, D. Guo, J. Qin, M. Cao, *RSC Adv.* **7**, 50812 (2017).
- [9] Q. Wang, N. Wang, S. He, J. Zhao, J. Fang, W. Shen, *Dalt. Trans.* **44**, 12878 (2015).
- [10] Z. Pan, Z. He, J. Hou, L. Kong, *Small* **19**, 2302788 (2023).
- [11] Y. Moritomo, M. Sarukura, H. Iwaizumi, I. Nagai, *Batteries* **9**, 393 (2023).

- [12] M. Pyrasch, A. Toutianoush, W. Jin, J. Schnepf, B. Tieke, *Chem. Mater.* **15**, 245 (2003).
- [13] E. Coronado, *Nat. Rev. Mater.* **5**, 87 (2020).
- [14] Y. Huang, S. Ren, *Appl. Mater. Today* **22**, 100886 (2021).
- [15] S. Ohkoshi, T. Iyoda, A. Fujishima, K. Hashimoto, *Phys. Rev. B* **56**, 11642 (1997).
- [16] A. Kumar, S.M. Yusuf, L. Keller, J.V. Yakhmi, J.K. Srivastava, P.L. Paulose, *Phys. Rev. B* **75**, 224419 (2007).
- [17] S. Ohkoshi, A. Fujishima, K. Hashimoto, *J. Am. Chem. Soc.* **120**, 5349 (1998).
- [18] M. Mizuno, S.I. Ohkoshi, K. Hashimoto, *Adv. Mater.* **12**, 1955 (2000).
- [19] M. Yamada, M. Arai, M. Kurihara, M. Sakamoto, M. Miyake, *J. Am. Chem. Soc.* **126**, 9482 (2004).
- [20] M. Fitta, H. Prima-Garcia, P. Czaja, T. Korzeniak, M. Krupiński, M. Wojtyniak, M. Bałanda, *RSC Adv.* **7**, 1382 (2017).
- [21] D.M. Pajerowski, J.E. Gardner, D.R. Talham, M.W. Meisel, *New J. Chem.* **35**, 1320 (2011).